

TIMESAFE: Timing Interruption Monitoring and Security Assessment for Fronthaul Environments

Joshua Groen, Simone Di Valerio[†], Imtiaz Karim[‡], Davide Villa, Yiwei Zhang[‡], Leonardo Bonati, Michele Polese, Salvatore D'Oro, Tommaso Melodia, Elisa Bertino[‡], Francesca Cuomo[†], Kaushik Chowdhury^{*}



arXiv:2412.13049v1 [cs.NI] 17 Dec 2024

Abstract—5G and beyond cellular systems embrace the disaggregation of Radio Access Network (RAN) components, exemplified by the evolution of the fronthaul (FH) connection between cellular baseband and radio unit equipment. Crucially, synchronization over the FH is pivotal for reliable 5G services. In recent years, there has been a push to move these links to an Ethernet-based packet network topology, leveraging existing standards and ongoing research for Time-Sensitive Networking (TSN). However, TSN standards, such as Precision Time Protocol (PTP), focus on performance with little to no concern for security. This increases the exposure of the open FH to security risks. Attacks targeting synchronization mechanisms pose significant threats, potentially disrupting 5G networks and impairing connectivity.

In this paper, we demonstrate the impact of successful spoofing and replay attacks against PTP synchronization. We show how a spoofing attack is able to cause a production-ready O-RAN and 5G-compliant private cellular base station to catastrophically fail within 2 seconds of the attack, necessitating manual intervention to restore full network operations. To counter this, we design a Machine Learning (ML)-based monitoring solution capable of detecting various malicious attacks with over 97.5% accuracy.

1 INTRODUCTION

Recent advancements in 5G and beyond have focused on disaggregating the Next Generation Node Base (gNB) and core networks, leading to the evolution of more open and modular systems. As a result, the fronthaul (FH) has emerged as a critical component, enabling the separation of radio elements from baseband processing. Disaggregated FH deployments were originally based on the Common Public Radio Interface (CPRI). While CPRI facilitated high-speed, centralized processing of radio signals, it lacked built-in security measures due to its design for single-vendor, co-located deployments [1]. The subsequent enhanced CPRI (eCPRI) introduced some security improvements, but significant gaps remain, particularly in synchronization [2]. The eCPRI-based O-RAN ALLIANCE's open FH now connects disaggregated components from multiple vendors, often using switched Ethernet topologies [3, 4]. While Ethernet's flexibility supports diverse traffic types, it

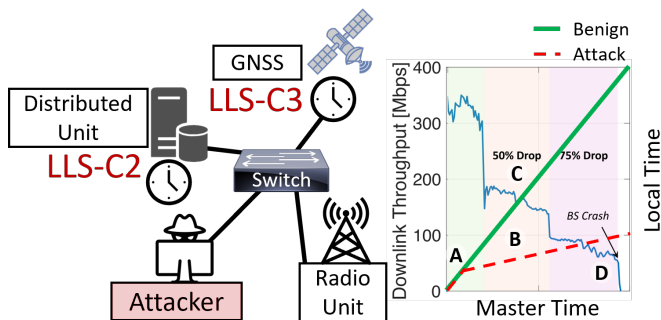


Fig. 1: The Open Fronthaul employs PTP to synchronize the master clock with distributed base station components over a switched network. In this scenario, an attacker compromises a device on the network and, at time A, initiates a Spoofing Attack. This leads to gradual synchronization drift (B), first degrading performance (C) and then causing the base station to crash at time D.

also exposes the FH to threats, as demonstrated by potential attacks on interconnected devices [5–9]. These attacks can disrupt synchronization and cause outages. For example, as shown in Fig. 1, an attacker that gains access to the FH network can carry out spoofing attacks that cause synchronization drift, resulting in a reduction in throughput and eventually a complete crash of the base station. Although there are ongoing efforts by industry, government, and academia to address these security gaps [1, 6, 10–13], no comprehensive standards for securing the FH have yet been established.

The open FH relies on precise timing through the Synchronization Plane (S-plane) to perform critical operations like OFDM synchronization, carrier aggregation, and handovers, which require time accuracy within tight margins [14, 15]. This synchronization depends on the Precision Time Protocol (PTP), which, like the FH, was initially developed without any security mechanisms [16]. While recent updates to the PTP standard include additional security features [17, Annex P], these have not been widely implemented in Open Radio Access Network (Open RAN) environments, leaving vulnerabilities that attackers could exploit.

Motivation and Scope. Security is critical for the success and widespread adoption of any system, and Open RAN

The authors are with: [†]Northeastern University; [‡]Sapienza University of Rome; ^{*}Purdue University; [†]University of Texas, Austin.

Corresponding author E-mail: groen.j@northeastern.edu.

This article is based upon work partially supported by U.S. National Science Foundation under grants CNS-1925601 and CNS-2112471 and by SERICS (PE00000014) 5GSec project under the MUR National Recovery and Resilience Plan funded by the European Union - NextGenerationEU.

has been criticized for lacking robust security mechanisms. In response, the O-RAN ALLIANCE established WG11 [11] to define a security framework, including zero-trust architectures [18], procedures, and defense mechanisms essential for Open RAN’s success [13]. While WG11 acknowledges that attacks on the S-plane can have a high impact, they consider the likelihood low due to the perceived sophistication required by an attacker [19]. However, a significant gap remains in analyzing security risks and proposing solutions for the open FH S-plane in production-grade Open RAN environments. Many researchers lack access to realistic over-the-air systems for testing and validating both attacks and countermeasures. To address this, we developed a Digital Twin system that replicates our production-ready FH network environment, enabling rapid experimentation and analysis.

In this paper, we aim to: (i) confirm the high impact of PTP attacks in a production-ready, 5G and O-RAN-compliant private cellular network; (ii) demonstrate that these attacks require relatively low sophistication to execute successfully; (iii) provide a Digital Twin framework for further analysis of attacks and development of solutions; and (iv) develop and evaluate detection mechanisms, showing that our Machine Learning (ML) model can effectively identify malicious PTP attacks with over 97.5% accuracy across diverse environments.

Contributions. Based on this motivation, we propose TIMESAFE: Timing Interruption Monitoring and Security Assessment for Fronthaul Environments, a comprehensive framework for assessing the impact and likelihood of attacks against PTP in the FH of Open RAN and 5G networks. TIMESAFE utilizes machine learning to enhance monitoring and provide highly accurate attack detection. The main contributions of our work include:

- **Experimental Analysis:** We conduct the first experimental analysis of the impact of timing attacks in a production-ready private cellular network (see Table 2), following O-RAN ALLIANCE procedures [20]. Our findings reveal that these attacks can lead to catastrophic outages of the gNB, highlighting critical vulnerabilities in PTP synchronization mechanisms.
- **Attack Demonstration:** We show that timing attacks on PTP in the FH S-plane are straightforward and require minimal sophistication, countering the belief that such attacks are highly complex.
- **Machine Learning Detection:** We develop a state-of-the-art transformer-based ML detection mechanism, achieving over 97.5% accuracy in detecting attacks on a deployed Distributed Unit (DU).
- **Open Source and Dataset Contributions:** Upon acceptance, we will open source our framework, including our Digital Twin design, the attacks, ML models, automation scripts, and a .pcap traffic trace dataset, to support further research and advancement in O-RAN security.

Responsible Disclosure. We have disclosed the identified attacks to the O-RAN ALLIANCE Working Group 11 (O-RAN-CVD-002, O-RAN-CVD-003). Our commitment extends beyond this; we are dedicated to collaborating with regulatory organizations and product vendors to enhance security. Through this proactive approach, we aim to en-

sure the robustness and resilience of the FH against future threats.

The rest of the paper is organized as follows. In Section 2, we provide background on the S-plane and PTP, while Section 3 surveys prior work. Next, we describe the threat model in Section 4 and our test beds in Section 5. We show the impact of the attacks in Section 6. Then, we demonstrate the need for ML based PTP monitoring tool in Section 7, describe our model in 8 and show state of the art results in Section 9. Finally, we provide additional insights and directions for research in Section 10, and draw our conclusions in Section 11.

2 BACKGROUND

Traditional Radio Access Network (RAN) architectures are monolithic, leading to vendor lock-in and limited flexibility. The Open RAN paradigm addresses these issues with disaggregated, software-based components and open interfaces [21], based on the 3GPP 7.2 split between Radio Unit (RU) and DU. Current O-RAN/ETSI standards [3, 4] do not mandate encryption on the FH interface due to bandwidth and latency concerns [13], though some studies suggest using Media Access Control Security (MACsec) for added security [5, 22, 23]. We start by defining key acronyms in Table 1, followed by background on the S-plane, PTP, and security.

Acronym	Definition
PTP	Precision Time Protocol
FH	Fronthaul
DU	Distributed Unit
RU	Radio Unit
ML	Machine Learning
O-RAN	Open Radio Access Network
S-plane	Synchronization Plane
UE	User Equipment (e.g., mobile phone)
gNB	Next Generation Node B (5G base station)
BMCA	Best Master Clock Algorithm
LLS-C	Lower Layer Split Control Plane

TABLE 1: Glossary of commonly used acronyms.

2.1 Fronthaul S-plane

The FH S-plane standards define four clock model and synchronization topologies based on the Lower Layer Split Control Plane (LLS-C): LLS-C1, LLS-C2, LLS-C3, and LLS-C4 [3], as illustrated in Fig. 2. LLS-C1, where the DU and RU are directly connected without a switched network, poses the least security risk due to the absence of intermediate attack vectors. LLS-C4 provides timing directly to the DU and RU using local GNSS receivers, reducing PTP attack opportunities, except for potential GNSS jamming.

In contrast, LLS-C2 and LLS-C3 are more vulnerable due to their reliance on the switched network for PTP message transport. In these scenarios, every device in the switched network represents a potential attack vector. In LLS-C2, the DU is part of the synchronization chain to the RU with one or more Ethernet switches in between. LLS-C3 differs in that the DU is not in the synchronization chain; instead, timing is distributed from the Primary Reference Time Clocks (PRTC) to the DU and RU(s) through the network. The increased

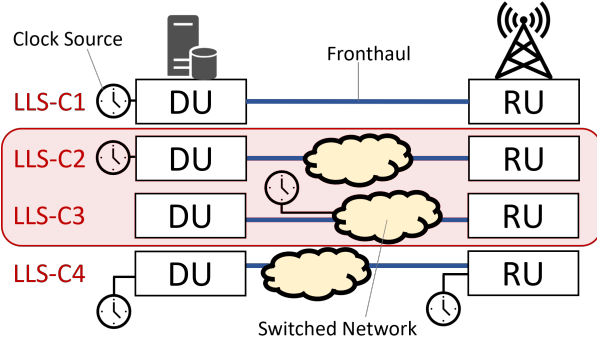


Fig. 2: The Fronthaul connects the Distributed Unit (DU) to the Radio Unit (RU). There are four Synchronization Plane topologies based on the location of the clock source and switched network. LLS-C2 and LLS-C3 present the greatest risk to PTP because the switched network is used to transport the timing messages.

complexity and multiple entities involved in securing the network infrastructure expand the risk surface, making LLS-C2 and LLS-C3 the most susceptible to attacks [19, 24].

2.2 PTP Overview

The PTP standard (IEEE 1588 [25]) ensures precise network clock synchronization in the nanosecond range. It achieves this through hardware time stamping, which minimizes delays from the networking stack [26]. The process involves electing a master clock that synchronizes all slave clocks in the network through a series of exchanges and messages.

- **Best Master Clock Algorithm (BMCA).** The initial step in PTP involves leader election through the BMCA. During this process, each clock periodically broadcasts *Announce* messages that contain up to nine attributes, which help determine the best clock for master selection. Key attributes include:

- *Priority1*: A configurable priority setting used as the first comparison feature in the selection process.
- *ClockClass*: Indicates the clock's traceability and suitability as a time source.
- *ClockAccuracy*: Reflects the clock's precision.
- *ClockIdentity*: A unique identifier for the clock, used to resolve ties.

Each clock evaluates the *Announce* messages based on the available attributes, selecting the clock with the highest quality as the master. This process is dynamic, allowing for continuous re-evaluation and re-selection if higher-quality clocks are introduced or current attributes change.

- **Time Synchronization Process.** After being elected, the master clock begins the synchronization process with the slave clocks. *Frequency*, *Phase* and *Delay* are critical aspects that influence synchronization.

Frequency refers to the rate at which a clock oscillates. To adjust the frequency, the master clock sends a *Sync* message and takes a timestamp (T_1). There are two types of clocks: *OneStep* clocks, which insert the timestamp (T_1) directly into the *Sync* message, and *TwoStep* clocks, which send a *FollowUp* message containing the timestamp (T_1). In the *TwoStep* case, the initial *Sync* message has an estimated

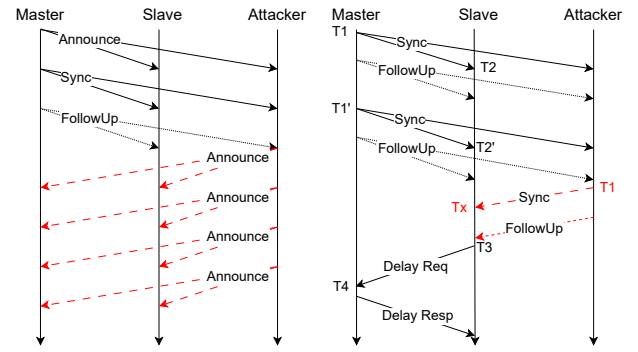


Fig. 3: The black (solid/dotted) lines represent normal traffic, while the red (dashed) on the left side illustrates the flow of messages during a Spoofing Attack, where an attacker manipulates the BMCA to become the master. The red (dashed) on the right side illustrates the flow of messages during a Replay Attack, showing the re-transmission of Sync and FollowUp messages.

timestamp or a value of 0. When the slave node receives the *Sync* message, it takes a timestamp (T_2). No timestamp is taken when the *FollowUp* message is received.

This process is repeated periodically and new timestamps (T_1' and T_2') are taken again as shown in Fig. 3. After receiving two *Sync* messages, the Slave can calculate the frequency difference relative to the Master clock, which is called $Drift = \frac{(T_2' - T_2) - (T_1' - T_1)}{T_1' - T_1}$. By calculating this drift, the Slave can adjust its own frequency to align with the Master clock, ensuring precise synchronization. To meet all FH timing requirements, additional Physical Layer Frequency Support (PLFS) support, such as SyncE, is required.

Delay refers to the time it takes for a message or signal to travel from one clock to another through the network. In general, delay can be computed via two mechanisms: (i) the *E2E* mechanism which measures the delay from the master to the slave; and (ii) the *P2P* mechanism which measures the delay between any two nodes irrespective of their role. E2E does not require intermediate nodes to be PTP aware, while P2P requires all intermediate switches to be PTP aware. In our experiments, we use the E2E mechanism, which is the default configuration. In this case, the master sends a *Sync* (and optional *FollowUp*) message and takes the timestamp (T_1). The slave receives the *Sync* message, takes the timestamp (T_2), sends a *DelayReq* and takes the timestamp (T_3). The master receives the *DelayReq* message and takes the timestamp (T_4) and stores it. Lastly, the master sends a *DelayResp* message with the timestamp (T_4). After receiving the *DelayResp* message from the master, the slave can measure the delay between the two nodes: $Delay = \frac{(T_4 - T_1) - (T_3 - T_2)}{2}$. This process, also shown in Fig. 3, is repeated at defined intervals.

Phase refers to the relative alignment of the waveform or signal between two clocks. In PTP, phase synchronization ensures that the phase difference between the master clock and the slave clock is minimized, allowing them to maintain consistent timing. After calculating the delay, the slave can also measure the phase, also called $Offset = (T_2 - T_1) - Delay$.

2.3 PTP Security

The original PTP standard, first published over twenty years ago, did not include any security mechanisms [16]. Subsequent revisions added a security annex, updated in 2019, detailing a flexible, multipronged security approach [25].

- **Prong A** focuses on authentication through an optional Type, Length, Value (TLV) field, with key management occurring outside of PTP. Adding cryptographic functions increases computational cost and processing latency, requiring synchronization adjustments, particularly in resource-constrained environments like FPGA-based RUs.
- **Prong B** addresses external security mechanisms, including MACsec (Layer 2) and IPsec (Layer 3). However, O-RAN Alliance specifications [3] and ITU-T G.8275.1 [27] generally do not permit IP transport. Using MACsec poses challenges; software implementations create virtual interfaces that disrupt hardware timestamping, reducing accuracy significantly. Although hardware-based MACsec solutions have been proposed [28, 29], they increase costs, delay, and complexity, reducing the virtualization central to Open RAN.
- **Prong C** focuses on redundancy (e.g., multiple grandmasters, alternate paths) to mitigate attacks and enhance system resilience. While beneficial, these methods add cost and complexity, conflicting with the push for increased virtualization and decreased costs in Open RAN [21].
- **Prong D** emphasizes monitoring and management. Monitoring PTP performance can help detect potential security attacks [25]. The annex suggests parameters to monitor, but does not specify actions to take upon detecting threats. Given the costs associated with the other prongs, it is logical to implement these security measures only when an attack is detected.

3 RELATED WORK

There is a growing awareness of the need to secure PTP. Several attacks are demonstrated in a data center context by DeCusatis *et al.* [30]. Itkin and Wool developed a detailed analysis of threats against PTP and proposed using an efficient elliptic-curve public-key signature for Prong A [31]. Shereen *et al.* [32] experimentally evaluated implementing Prong A, finding that software-based authentication adds at least an additional $70\mu\text{s}$ of delay. Similarly, Rezabek *et al.* [26] evaluated software-based authentication and concluded that there is visible degradation of clock synchronization for each hop in the network with standard deviations between 118 and 571ns.

There are several works that investigate security threats and propose related defense mechanisms for PTP in smart grids. Moussa *et al.* [33] proposed adding a new type of PTP clock and modifying the PTP slave functionality. Then in subsequent work, Moussa *et al.* proposed adding further message types to aid in detection and mitigation [35], and adding feedback from both slaves and master clocks to a reference entity [34].

A method targeting Prong C, where clock and network path redundancy are added, is proposed by Shi *et al.* [16]. Likewise, the approach by Finkenzeller *et al.* [36] uses redundant, or cyclic paths, to detect and mitigate time delay attacks.

Maamary *et al.* give an overview of several threats to the FH S-plane and discuss possible countermeasures [15], though they do not implement either attacks or countermeasures. FH security considerations are further described and MACsec is proposed as a solution by Dik *et al.* [5, 22, 28, 29]. While these works are the most similar to ours, they primarily address Prong B and could be implemented in parallel to our work.

In contrast to the above works, our paper is the first to demonstrate successful attacks against PTP used for the S-plane causing the gNB to fail and demonstrating how O-RAN-connected devices can be leveraged as attack vectors. We also are the first to propose a ML-based method to monitor PTP in accordance with Prong D, successfully discriminating between benign and malicious traffic with over 97.5% accuracy.

4 THREAT MODEL

The attack scenario we consider for both the production-ready network and digital twin environment is shown in Fig. 1. In this setup, a switched network connects a software-based DU, with robust computational and storage capabilities (e.g., an edge server running an open-source network stack), to a more limited RU, such as an FPGA-based device. The complexity of the Open RAN architecture, with its many interconnected components, heightens security risks [37]. Although the fronthaul network is protected by IEEE 802.1X, adversaries may bypass this security in a variety of ways.

- **Increased Remote Access.** With its open and multi-vendor architecture, O-RAN relies on a diverse range of suppliers, developers, and service providers, each with varying levels of access and control over networked components. As a result, the number of personnel who can potentially access sensitive infrastructure grows, increasing the risk of misconfigured or compromised authentication processes. IBM's X-Force Threat Intelligence 2023 report identified misuse of valid credentials (36%) and plaintext credentials on endpoints (33%) as common initial access vectors in cloud environments [38]. Such vulnerabilities are particularly concerning in O-RAN, where distributed network functions and the involvement of multiple parties create more opportunities for configuration errors and unauthorized access to the DUs [6, 39].

- **Increased Physical Access.** The distributed nature of gNB edge servers, often located in accessible public spaces such as sidewalks, rooftops, or building basements, makes on-site physical access an increasingly viable entry point for attacks on the FH [40]. Physical proximity to fronthaul infrastructure lowers the barrier for potential attackers compared to centralized cloud data centers. Once on-site, an adversary can bypass 802.1X by inserting a rogue device (e.g., a mini PC) into the network to intercept, modify, or replay traffic over already authenticated connections.

- **Dependency and Supply Chain Vulnerabilities.** Software-based network functions in 5G, including those in Open RAN, are susceptible to supply chain attacks, particularly with the use of unvetted and globally sourced components. A recent government report highlighted that supply chain risks from untrusted hardware and software vendors

Paper	Domain	Attacks Implemented	Mitigation Implemented	Type of Validation
[30]	Data center	Spoofing, Comp. Master Clock	None	Experimental testbed
[31]	None	Spoofing, Comp. Master Clock	Prong A, Modifications to PTP	Experimental testbed
[32]	None	None	Prong A	Experimental testbed
[26]	None	None	Prong A	Experimental testbed
[33–35]	Smart Grid	Spoofing, Replay	Modifications to PTP	Formal model verification
[16]	IoT	Spoofing	Prong C, Modifications to PTP	IoT testbed
[36]	None	Spoofing	Prong C, Modifications to PTP	Experimental testbed
[15]	O-RAN	None	None	None
[5, 22, 28, 29]	O-RAN	None	Prong B	Experimental testbed
TIMESAFE	O-RAN	Spoofing, Replay	Prong D	Production-ready network

TABLE 2: Overview of prior work on PTP security highlighting the application domain studied, the attacks (see Sec. 4.1) and mitigations implemented, and the framework used for validation. Our work is the first to demonstrate the impact of attacks on an O-RAN production-ready environment as well as the first to implement a Prong D (monitoring and management) solution.

are significant threats, as adversarial actors could embed backdoors in either the DU or RU to manipulate fronthaul traffic without being detected by 802.1X [40]. Recent studies of several O-RAN software stacks (including those provided by the open-source projects in the O-RAN Software Community) have uncovered numerous high-risk dependencies, misconfigurations, and weak security practices, such as inadequate access control, lack of encryption, and poor secret management across multiple components [7–9, 41, 42].

The combination of increased remote access to DUs and physical access to the FH, along with dependency and supply chain vulnerabilities, makes gaining access to a device connected to the FH network not just plausible but increasingly likely. Once an attacker gains access to a device on the switched network, they can observe, replay, or inject PTP broadcast packets sent through the switch.

4.1 Attack Methods

Here we highlight a few of the possible attacks that can compromise PTP synchronization.

- **Denial-of-Service (DoS) Attack.** A DoS attack floods the network with a high density of PTP messages or other types of traffic, overwhelming PTP nodes and preventing them from correctly processing timing messages.
- **Spoofing Attacks.** In a spoofing attack, an adversary sends malicious PTP messages to deceive slave clocks into accepting fake timing information. This method involves impersonating the master clock by sending fake Announce packets or sending false Sync, FollowUp, DelayReq, or DelayResp messages to disrupt legitimate synchronization among nodes in the network.
- **Compromised Master Clock.** A compromised master clock poses a severe threat to the PTP service, granting attackers control over the network’s synchronization source. Attackers can take control of the master clock by exploiting supply-chain vulnerabilities or gaining unauthorized access, enabling manipulation of timing messages and disruption of network operations.
- **Replay Attack.** A replay attack in PTP involves capturing and retransmitting timing messages, causing devices to synchronize with outdated or modified timestamps. This scenario can disrupt the accuracy of time synchronization and compromise the integrity of time-sensitive operations.

Within the TIMESAFE framework, we focus on two specific attacks targeting PTP synchronization: *Spoofing Attack* and *Replay Attack*. These attacks are chosen for their

direct impact on PTP synchronization mechanisms. The spoofing attack manipulates the BMCA to influence master clock election, affecting network-wide synchronization. The replay attack disrupts time synchronization by altering drift, offset, and delay calculations on slave clocks. Details of these attacks are illustrated in Fig. 3 and discussed in the following sections. Other attack types, such as DoS and compromised master clock attacks, involve vulnerabilities beyond PTP itself.

4.1.1 Spoofing Attack

The TIMESAFE framework spoofing attack targets PTP nodes by sending counterfeit Announce messages to manipulate the BMCA leader election and assume the role of the master clock. Initially, the attacker monitors benign traffic to gather critical information about the protocol configuration and node attributes. With this data, the attacker crafts Announce packets designed to have superior attributes crucial for master clock selection. The BMCA relies on up to nine features to determine the master clock, starting with *Priority1* (Sec. 2.2). The attacker manipulates this value by setting it to 1. Similarly, the attacker sets the values for *ClockClass* to 1. The *ClockIdentity* field is created by inserting priority values between the manufacturer ID and device ID portions of the MAC address. The attacker inserts `ffff` ensuring it has higher priority values than the legitimate Master. Other values are copied from the legitimate master.

These crafted messages are sent periodically to maintain the attacker’s role as master. Apart from Announce messages, no synchronization packets are sent, and DelayReq messages from slaves remain unanswered. By disrupting the synchronization process, all clocks operate independently, leading to a gradual drift. Consequently, the attacker introduces synchronization errors among all nodes in the network, causing a complete outage for the gNB, as we will show in Section 6.1 and illustrated in Fig. 1.

4.1.2 Replay Attack

The Replay Attack involves sniffing time synchronization messages (Sync and FollowUp) from the Master clock, storing, and retransmitting them after a delay. When the Slave clock receives the retransmitted messages, it uses the outdated timestamp T_1 and a new timestamp T_x to compute drift, delay, and offset (see Fig. 3). The formulas in Sec. 2.2 become: $Drift = \frac{(T'_2 - T_x) - (T'_1 - T_1)}{T'_1 - T_1}$, $Delay = \frac{(T_4 - T_1) - (T_3 - T_x)}{2}$, and $Offset = (T_x - T_1) - Delay$. The actual difference

between when T_1 is generated and received in the malicious PTP message significantly exceeds the calculated difference, causing offset to increase by orders of magnitude and severely disrupting network synchronization, as we will detail in Section 6.2.

5 EXPERIMENTAL TEST BEDS

For TIMESAFE, we use two experimental test beds to assess network timing interruption attacks, analyze PTP security measures in Open RAN networks, and evaluate malicious PTP detection systems on the DU. The first test bed is a production-ready 5G network, while the second is a dedicated Open RAN digital twin environment for rapid testing, prototyping, and developing attacks and solutions.

5.1 Production-Ready Network

Our first experimental analysis is performed on a private 5G network, deployed at Northeastern University [43] comprising 8 NVIDIA Aerial RAN CoLab (ARC) nodes, with dedicated Core Network (CN) and FH infrastructure. We utilize this production-ready platform to capture traffic and evaluate attacks on an O-RAN and 5G-compliant system based on a 3GPP 7.2 split, with a combination of open-source components for the higher layers of the stack, as well as commercial devices for the fronthaul infrastructure and the radios [3].

NVIDIA ARC combines the open-source project OpenAirInterface (OAI) [44] for the higher layers of the protocol stack with NVIDIA Aerial, a physical layer implementation accelerated on Graphics Processing Unit (GPU) (NVIDIA A100) and with a 7.2 implementation that combines NVIDIA Mellanox smart Network Interface Cards (NICs). In an ARC server, the GPU is coupled with the programmable NIC (a Mellanox ConnectX-6 Dx) via Remote Direct Memory Access (RDMA), bypassing the CPU for direct packet transfer from the NIC to the GPU. This architecture enables high-speed DU-side termination of the Open FH interface.

The FH infrastructure uses a Dell S5248F-ON switch and a Qulsar QG-2 as the grandmaster clock, distributing PTP and SyncE synchronization to the DU and RU with an O-RAN LLS-C3 configuration. For PTP synchronization, we use *ptp4l*, an IEEE 1588 compliant implementation for Linux that offers extensive configuration options and enables monitoring and logging of synchronization. The RU is a Foxconn 4T4R unit operating in the 3.7 – 3.8 GHz band, with Commercial Off-the-Shelf (COTS) 5G smartphones from OnePlus (AC Nord 2003) as User Equipments (UEs) [45].

While the DU codebase is open and potentially extensible to secure the S-Plane, the RU incorporates a closed-source FPGA-based termination for the FH interface, precluding additional security mechanisms in the FH environment from being directly enabled. Thus, we also adopt a trace-based approach similar to [13], configuring a port of the FH switch to mirror the FH traffic to a server running packet capture. Specifically, we capture all traffic traversing the FH for over 20 minutes under several different traffic loads.

5.2 Digital Twin Environment

To leverage these traces we built a digital twin environment using two desktop computers with Intel i9-13900K CPUs and NVIDIA Mellanox ConnectX-4 Lx NICs to represent the DU and RU, while a third desktop computer with an Intel Core i7-10700 CPU serves as the attacker. All machines are connected over a private, 10 Gbps capable switched network. Digital twins provide a highly accurate representation of the network and its devices, making them invaluable for designing and testing ML-based algorithms to detect malicious traffic and ongoing attacks [46]. Once trained, ML-based control solutions need to be validated and tested in controlled environments to avoid disruptions in production networks [47]. Our setup allows for rapid testing, prototyping, and the development of both attacks and solutions, ensuring robust security measures before deployment in real-world scenarios, meeting the need to test and evaluate any proposed S-plane security measures as discussed in [15]. We use `.pcap` files captured on the production-ready Open FH to accurately emulate the original FH and observe the impact the C and U plane traffic has on the PTP protocol operating in the S-Plane [13].

On top of the background traffic, we start PTP traffic between the DU and RU with *ptp4l*. This mirrors the setup in our production-ready network, which also uses *ptp4l* for PTP synchronization. We use the LLS-C2 profile in our digital twin environment, where the DU is the Master Clock and the RU is our Slave Clock. The attacker does not actively participate in the PTP protocol. Instead, it is capable of observing, replaying, or inserting PTP traffic. We discussed the details of our attacks in Section 4.1.

6 IMPACT OF THE ATTACKS

Implementing security measures incurs performance costs [13, 24, 48], so balancing attack risks with the cost of securing the system is crucial. We use the TIMESAFE framework to evaluate the impact of attacks on the S-plane within our test environments, following the O-RAN interfaces S-plane specification [20]. Our assessment focuses on the gNB's availability. According to NIST's National Vulnerability Database (NVD)[49], impact levels are categorized as none, low, or high. Low impact attacks cause performance degradation or intermittent availability without fully denying service, affecting functionalities like Carrier Aggregation and handovers[14]. High impact attacks, however, result in complete outages, denying service to all UEs.

6.1 Production-ready Network Impact

We test our attacks in the production-ready private 5G network to assess each attack's impact following the recently published guidelines in the O-RAN ALLIANCE testing specifications [20]. Based on our threat model in Section 4, we assume that one of the 8 DUs is the compromised machine.

In our initial tests, we found that switch configurations can provide protection against attacks. Malicious packets are not always received by other nodes, as verified through Wireshark captures on both the malicious machine and other nodes. This protection is tied to the switch port's PTP

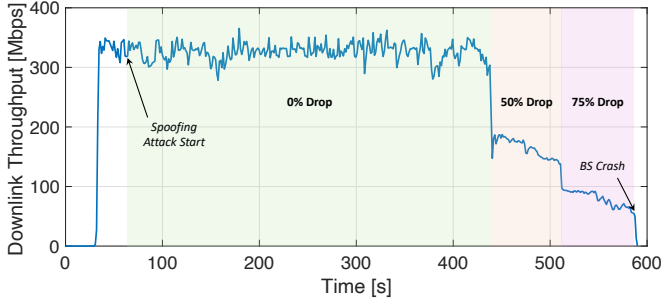


Fig. 4: Downlink throughput to a UE during a spoofing attack with the switch port set to PTP master. Approximately 60 seconds into the experiment, the spoofing attack is initiated. Around second 440 there is a 50% drop in throughput, progressing to a 75% drop by second 510, and ultimately causing the base station to crash at around second 580.

role settings. On the Dell S5248F-ON switch, ports set to master only send PTP packets, slave mode only receives, and dynamic mode allows both. Additionally, switch configurations can block duplicate MAC addresses. While a properly configured switch prevented our replay attack, assuming correct configurations is risky, especially when DU and RU vendors lack control over network settings, and the complexity and diversity of equipment and configurations in the FH path exacerbate this risk [38, 39, 50].

In our first successful attack, we configure the port of our malicious machine with a PTP master role. We start our private 5G network, connect the UE, and begin sending around 300 Mbps downlink iPerf traffic. After approximately 60 seconds, we launch the spoofing attack, as shown in Fig. 4. Monitoring the PTP service logs at the DU reveals that the attack causes the DU to lose synchronization with the grandmaster clock, leading to a drift in network synchronization as the DU uses its internal clock. This drift degrades UE performance, eventually causing disconnection from the network. About 380 seconds after the beginning of the attack, there is a sudden 50% drop in throughput. From this point, the throughput continues to drop roughly linearly as the clock drift increases. Finally, the DU loses synchronization with the RU, the throughput drops to 0, and the UE disconnects. When this attack stops, the DU resynchronizes with the grandmaster clock, and the network returns to a healthy state.

Next, we configure all ports as PTP dynamic so that malicious packets can be received by the other nodes and repeat the experiment. This time, the malicious PTP packets reach all the machines in the network. Approximately 2 seconds after the attack begins, the RU crashes, stopping its operations, causing the 5G cell to drop and the UE to lose connection, as shown in Fig. 5. While the DU was able to recover on its own after the first attack, the RU required a manual reboot to regain functionality after the second attack. This behavior might be device specific, in our case the Foxconn RU. Regardless of any potential vendor-specific variations, these attacks proved to be very powerful, causing significant disruption and necessitating manual intervention to restore full network operations. These tests demonstrate

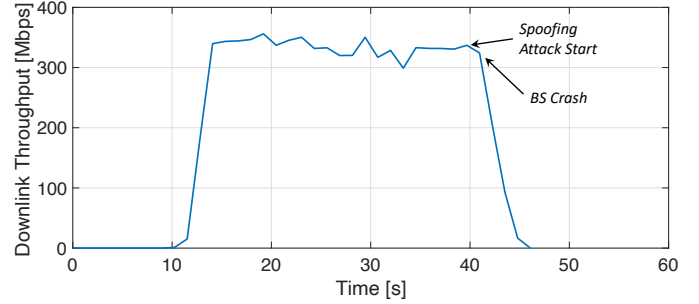


Fig. 5: Downlink throughput to a UE during a spoofing attack with switch ports set to PTP dynamic role. Throughput remains stable at around 350 Mbps initially. About 40 seconds in, the spoofing attack begins, causing the 5G cell to drop and the UE to lose connectivity.

the impact to the Open RAN gNB is *high*. Failing to secure the S-plane against spoofing attacks results in a complete outage of the gNB.

6.2 Digital Twin Network Impact

Next we tested the impact of our attacks on PTP functionalities in the Digital Twin environment, focusing on disruptions to synchronization and leader election rather than effects on the UE. We employed cyclic attack/recovery patterns with durations of 30/30, 40/20, 50/10 seconds, and continuous attacks for both of the attacks discussed in Sec. 4.1. The attack duration is the period (in seconds) the attack is carried out, while during the recovery time no attack occurs allowing PTP synchronization to recover. Each experiment involved four background traffic traces, resulting in 32 tests with durations ranging from 120 to 450 seconds, depending on the traffic. Results from the RU confirm significant performance degradation in PTP, with varying severity of impact. Here we briefly highlight the effectiveness of both attacks.

Spoofing Attack: Fig. 6 shows the impact of the 50/10 (50 s attack, 10 s recovery) spoofing attack. Synchronization is disrupted whenever the attacker becomes the master clock, causing the RU to rely on its internal clocks, leading to synchronization drift. The impact of this attack depends on the accuracy of each device's internal clock as well as the length of time of the attack. The observable spike in delay is actually reported shortly after the attack ends, when the legitimate master and slave begin synchronizing again. This spike shows the amount of synchronization drift that occurred during the attack. While there is some natural variation in delay due to the background traffic, shown in light green in Fig. 6, the announce attack (dark red) shows synchronization drift can exceed 40,000 ns.

Replay Attack: This attack has a more severe impact on node synchronization, as shown in Fig. 7, where we display the results of the 30/30 s cycle. Normally, delay values range between 25 and 45 nanoseconds, but during the Replay attack, these values spike by several orders of magnitude, peaking at over 20 million nanoseconds. Comparing Fig. 6 and Fig. 7 it is evident that the replay attack is more disruptive than the spoofing attack, causing a high synchronization

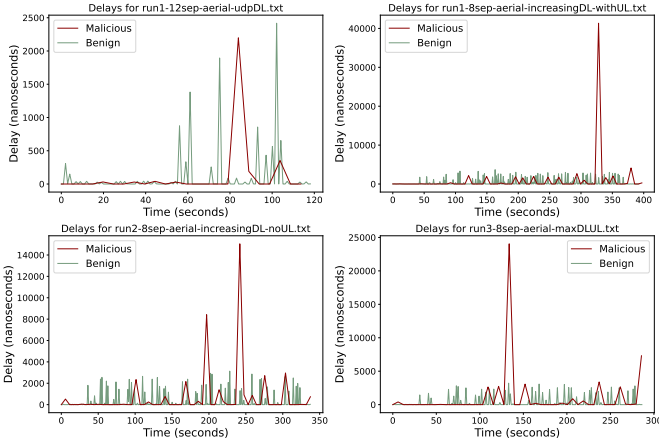


Fig. 6: The drift caused by the spoofing attack (dark red) can exceed 40,000 ns, exceeding normal background traffic (light green). During the 50-second spoofing attack period, the RU relies on its internal clocks. When the 10-second recovery period begins, a large spike in calculated delay represents the synchronization drift caused by the attack.

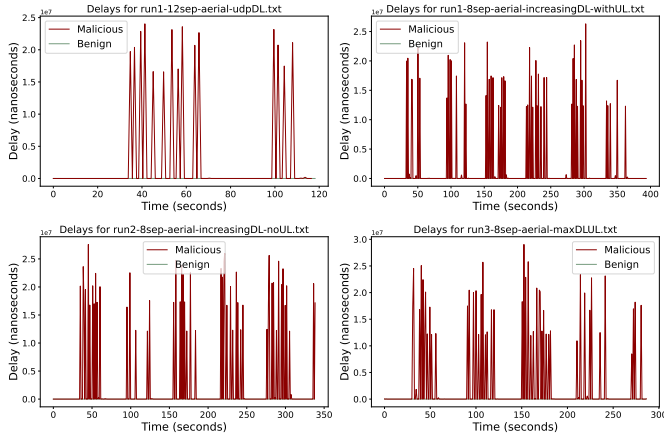


Fig. 7: The delay values during the 30-second replay attack (dark red) spike to over 20 million nanoseconds, compared to normal background traffic (light green). The replay attack causes a much higher synchronization drift more quickly than the spoofing attack, and it takes longer for PTP to recover.

drift more quickly and requiring more time for PTP to fully recover.

7 NEED FOR ML BASED DETECTION

As shown in Section 6, synchronization attacks can have catastrophic consequences, including complete outages of the gNB. However, the virtualized, multi-vendor nature of Open RAN and the high precision required for synchronization over the S-plane create challenges for implementing traditional security measures. While hardware-based solutions like MACsec can provide security, they introduce additional costs and complexity to the resource-constrained RU [28, 29].

To address these limitations, we propose a monitoring system (Prong D) within the DU, which has more computa-

tional resources and flexibility. Given the complexity and variety of potential attacks on synchronization protocols, simple rule-based or threshold mechanisms are insufficient. Instead, ML offers a more adaptive approach for several reasons.

- **Rule-Based Solutions:** Developing rule-based solutions requires extensive expert knowledge to create specific rules for every potential attack. In Sec. 7.1, we outline the complexity involved in designing expert rules to detect even just two types of attacks.

- **Fixed Thresholds:** Rule-based solutions often rely on fixed thresholds, which are challenging to determine optimally. Even with well-designed thresholds, these methods are limited in their ability to adapt to new or evolving threats. In contrast, ML models do not require setting fixed thresholds. As we will show in Sec. 9.2, well designed models exhibit resilience against reshaped attacks.

- **Flexibility:** In contrast to rule-based approaches, a well-trained ML model can generalize across various attack types. For instance, we created a new DoS attack by sending a high rate of random or invalid PTP messages. Although this attack did not disrupt PTP timing, it still indicated malicious activity. Our ML model, despite not being specifically trained on this attack, correctly identified over 66% of the malicious traffic, whereas the heuristic model failed completely. This shows that TIMESAFE’s ML-based solution is highly flexible and capable of detecting sophisticated, unpredictable attacks.

- **Accuracy.** An effective monitoring solution must deliver accurate results. As we will demonstrate in Sec. 9.1, our ML model significantly outperforms the rule-based approach, achieving 99% accuracy in a production environment.

Rule-based systems such as those described in [25] struggle to keep pace with the wide range of attacks, while other heuristic methods require additional clocks or changes to the physical infrastructure [16, 33, 36]. Additionally, legitimate changes in master clocks, changes in network topology, and sequence number resets can often resemble malicious activity, complicating detection efforts. ML models excel at identifying patterns and anomalies within large datasets, enabling them to distinguish between benign fluctuations and actual threats. By leveraging ML, we can develop robust monitoring systems capable of adapting to new and evolving attack vectors, ensuring reliable network performance and security.

7.1 Heuristic Detection Results

To highlight the challenges of rule-based systems, We developed a heuristic model to detect attacks using a set of predefined rules.

Spoofing Attack: This attack sends numerous `Announce` packets to become the master and disrupt synchronization. Our heuristic detects this by monitoring the number of adjacent `Announce` packets. Typically, no more than 2 adjacent `Announce` messages are seen in normal traffic. If the heuristic detects 4 or more consecutive `Announce` packets, it flags an attack.

Replay Attack: This sophisticated attack replays benign `Sync` and `FollowUp` packets with delays, mimicking legitimate traffic. Detection relies on the Sequence ID and Message Type, looking for anomalies like `Sync` and `FollowUp`

True Label	0	99.47%	0.53%
	1	82.20%	17.80%
		0	1
		Predicted Label	

Fig. 8: Confusion matrix of the heuristic solution for detection of PTP attacks showing an extremely high FN rate.

messages separated by other packets, Sequence ID values lower than previous packets, and duplicates. The heuristic uses a queue of the last S packets to identify these issues, but this method may strain memory resources.

Testing under the same conditions we use in Section 9.2 showed that while the heuristic effectively detects `Announce` attacks, it struggles with overall accuracy. The primary issue is its sensitivity to individual packets: legitimate packets observed during an attack can reset the heuristic, causing it to miss subsequent malicious packets. Results, as shown in Fig. 8, indicate poor overall performance due to these limitations.

8 TIMESAFE ML-BASED DETECTION

Traditional heuristic methods are inadequate for detecting all types of malicious packets, given the dynamic and adaptive nature of cyberattacks. Instead, a ML approach is better suited to capture the temporal dependencies and patterns in PTP data. PTP packets, characterized by features such as Ethernet addresses, sequence IDs, message types, and inter-arrival times, form a high-dimensional feature space where subtle anomalies may occur. Unlike rule-based systems, ML models can learn these complex patterns and correlations to identify potential malicious activity.

8.1 ML Model Selection

We used our digital twin environment to generate training data, as described in Sec. 6.2. The data was split into equal-sized chunks (1000 messages each) without overlaps. We randomly selected 80% of the chunks for training, 10% for validation, and 10% for testing. Upon acceptance, we will open-source our complete data set and training pipeline.

We initially evaluated a wide range of ML models, as shown in Table 3, using the same test traces for all offline accuracy tests. All ML models tested had higher accuracy than the rule-based approach in Sec. 7.1. However, accuracy alone is not sufficient; the impact of False Negatives (FNs) (or missing an attack) is catastrophic, as shown in Section 6.1, while the impact of False Positives (FPs) is much lower. Therefore, we also examine each model’s recall. Given the clear performance advantage of the CNN and Transformer models, we selected both for further evaluation. The complete confusion matrices for the initial offline results for these models are shown in Fig. 9.

Our task of classifying packet sequences as malicious or benign parallels sentiment analysis and image classification, where context or spatial features are key. Just as sentiment analysis depends on word context and image classification on visual patterns, our models must capture subtle packet

Model	Accuracy (%)	Recall (%)
Heuristic	50.95	17.80
Linear Regression	75.70	17.90
KNN	79.91	51.49
Gradient Boosting Classifier	86.59	58.75
Random Forest	84.99	72.00
Decision Tree	84.26	72.45
LSTM	72.97	75.00
Naive Bayes	65.72	83.26
CNN	97.90	97.05
Transformer	97.99	98.33

TABLE 3: All machine learning models outperform the heuristic (rule-based) approach in both accuracy and recall on the offline dataset. The CNN and Transformer models achieve significantly higher performance than other methods.

True Label	0	99.15%	0.58%
	1	4.31%	97.05%
		0	1
		Predicted Label	

(a) CNN

True Label	0	97.49%	2.51%
	1	1.67%	98.33%
		0	1
		Predicted Label	

(b) Transformer

Fig. 9: Confusion matrices from initial offline testing for the CNN and Transformer.

sequence patterns. CNNs excel at extracting spatial features, making them effective at identifying key packet patterns, while transformers are superior in handling sequential data and capturing contextual dependencies. This capability to understand complex patterns intuitively explains why CNN and transformer models outperform others in detecting malicious PTP activities.

8.2 ML Model Description

Here we briefly describe the design of the two best performing models, the CNN and transformer. A complete description of each model along with code used will be made open source upon acceptance of this article. All the models use the same six input features, F : Ethernet source and destination addresses; packet size; PTP sequence ID; PTP message type; and inter-arrival time. The MAC address helps identify flows and packet direction. The PTP message type and sequence ID are crucial for understanding the nature and order of PTP messages, aiding in the detection of deviations from expected behavior. Packet length can indicate malformed or malicious packets with extra payload. Inter-arrival time, specified by the O-RAN ALLIANCE for both announce and sync messages, is another key indicator of potential attacks, though minor variations between packets are expected.

Our CNN model uses a 2D convolutional architecture to process input sequences of fixed length S ($S = 32$ for all results presented) and six features ($F = 6$), represented as a 1-channel image with dimensions corresponding to the sequence length and feature count. The model has two convolutional layers: the first uses 16 filters with a 3×3 kernel, followed by ReLU activation and 2×2 max pooling, reducing spatial dimensions. The second layer applies 32 filters with a 3×3 kernel, followed by ReLU and max

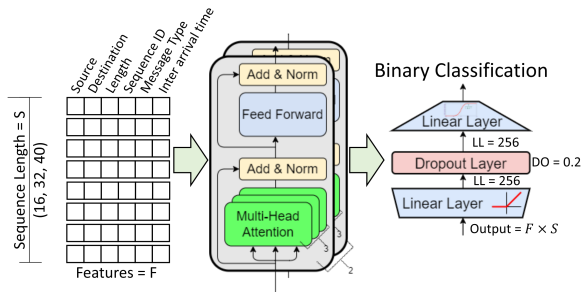


Fig. 10: The final TIMESAFE transformer model uses 2 transformer layers, a fully connected linear layer with ReLU activation function, a dropout layer, and a second linear layer with a sigmoid activation function. The output is a single binary classification for the entire sequence.

pooling. The output is flattened and passed through two fully connected layers with ReLU and sigmoid activations to produce a binary classification.

Our transformer-based model (see Fig. 10) uses only the encoder portion of a full transformer architecture. It processes input sequences with fixed lengths, varied during training and evaluation to include lengths of $S = \{16, 32, 40\}$ packets. These lengths balance the trade-off between incorporating more historical data (and requiring more memory) and improving accuracy and recall. We also treated the number of attention heads $\{2, 3\}$ as a hyperparameter with two configurations. The transformer encoder outputs a feature matrix of dimension $F \times S$, which is then fed into a fully connected linear layer with a ReLU activation function, followed by a dropout layer with a probability of 0.2 and a final linear layer with a sigmoid activation function. The model produces a single binary classification for the sequence.

For both the CNN and transformer models, we employed a custom Weighted Binary Cross-Entropy Loss function to address class imbalance and unequal error costs. However, since the initial setting of 1 for both weights yielded satisfactory results, we did not adjust these weights further. We used the Adam optimizer with an initial learning rate of 0.001 and configured a StepLR scheduler to reduce the learning rate by a factor of 0.1 every 10 epochs. Early stopping was enabled, with monitoring for validation loss improvement and a patience parameter set to 20 epochs.

8.3 Deploying TIMESAFE

To test our proposed solution, we built a detection pipeline with three parallel components: packet acquisition and filtering, pre-processing, and decision-making. The pipeline captures Ethernet frames, filters for PTP packets, and extracts key features, such as MAC addresses, length, sequence ID, message type, and inter-arrival timestamps. The pre-processing stage maps observed MAC addresses to integers, enabling the model to learn traffic patterns rather than specific addresses. The decision-making block uses a sliding window approach to classify each sequence as benign or malicious, using either an ML model or a rule-based algorithm. We use a stride of two for our sliding

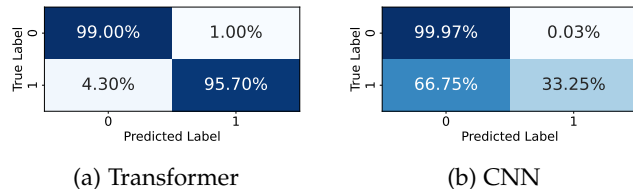


Fig. 11: Confusion matrices for production environment attack detection. The transformer greatly outperforms the CNN, showing it is able to adapt to new environments.

window, so at most two malicious packets are sent before our model detects the attack.

9 TIMESAFE DETECTION RESULTS

This section demonstrates that TIMESAFE accurately detects attacks in a production-ready 5G network and shows its resilience to reshaping attacks in our Digital Twin environment.

9.1 Production-ready Detection Accuracy

We evaluated the TIMESAFE detection pipeline using a trace (.pcap) captured during a successful attack in the production-ready environment, as illustrated in Fig. 5. The results demonstrate that the transformer model with 2 attention heads and a slice length of 32 significantly outperformed other transformer configurations, achieving an accuracy exceeding 99%. The confusion matrix in Fig. 11a illustrates the model's strong performance, highlighting its ability to accurately distinguish between malicious and benign traffic in a real-world setting.

In contrast, Fig. 11b shows that the performance of the CNN model was substantially degraded when applied to the new environment. This suggests that the CNN struggled to generalize to unseen data and failed to adapt to the subtle contextual variations present in the production environment. The transformer model, however, maintained its robustness, effectively identifying the nuanced patterns and indicators of the attack, even in a more complex and dynamic setting. This reinforces the transformer's ability to generalize well to new conditions, capturing intricate relationships across sequences that may vary from one environment to another.

9.2 Digital Twin Detection Accuracy

To further validate our ML model, we deployed TIMESAFE in a digital twin environment that simulates the production-ready network. This setup provides a realistic testbed for evaluating the model's performance under a wide variety of conditions. While running full PTP with *ptp4l*, we keep system time updates on the DU and attacker disabled, allowing us to log prediction outcomes with accurate DU timestamps. The attacker logs the attack type and its timestamps, enabling us to measure decision accuracy. Analysis reveals that we can detect attacks with just one or two malicious PTP packets reaching the DU.

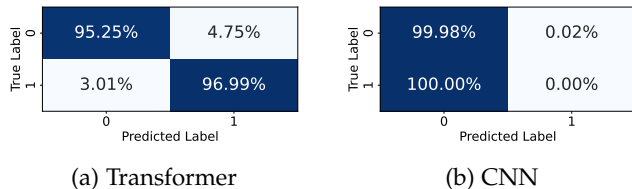


Fig. 12: Confusion matrices for evaluating resilience to reshaped attacks with randomized attack and recovery durations. The transformer shows resilience to this strategy change, while the CNN fails to generalize.

During the experiment, several tests were performed. At the start of each test, the DU, RU, and attacker exchanged initial messages to confirm readiness. Once prepared, they initiated a 5-minute test. Throughout the test, the DU continuously logged predictions with timestamps, while the attacker recorded the attack types, along with their start and end times, and the duration of both the attack and recovery phases. This cycle repeated for the entire test duration, alternating between attack and recovery phases. Recall that during training, we used cycles of 30/30, 40/20, 50/10 seconds, and continuous attack, as described in Section 6.2. To evaluate the models' ability to generalize to altered attack patterns, the attacker in this experiment randomly selected an attack duration from the continuous range [10, 30] seconds and a recovery duration from the continuous range [40, 60] seconds. The detection results from this experiment are shown in Fig. 12. The transformer demonstrated excellent resilience against the reshaped attack, while the CNN completely failed to detect it. This outcome highlights the transformer's robust ability to adapt to previously unseen attack strategies, confirming greater suitability for real-world deployment where attack patterns can be unpredictable.

10 DISCUSSION

The Open RAN framework's push towards increased virtualization and softwarization [51, 52] necessitates security solutions that align with this trend. Prong D (Sec. 2.3), which involves monitoring, is well-suited to the softwarized DU environment. However, future work should prioritize several additional key areas.

Attacks in Other Synchronization Topologies. Our focus on LLS-C2 and LLS-C3, due to their high vulnerability, does not encompass all risks. For instance, jamming GNSS signals could affect LLS-C4, and supply chain attacks on primary reference clocks pose additional threats. Network redundancy, as suggested in Prong C, enhances protection and resilience, potentially mitigating such threats through redundant paths and clocks [16, 36, 53, 54].

Additional Attacks Against PTP. While TIMESAFE currently addresses two types of attacks, other threats like packet removal and selective delay manipulation also merit investigation [15]. Expanding TIMESAFE to include multi-class classification for various attack types could refine threat detection and response strategies.

Authentication. Enhancing PTP security through authentication, as outlined in Prong A, is crucial. Implement-

ing digital signatures can verify message integrity and authenticity, preventing replay and spoofing attacks. However, integrating these mechanisms must balance security with the real-time performance needs of PTP in Open RAN. Efficient, lightweight cryptographic algorithms are essential to avoid introducing latency that disrupts timing synchronization. Additionally, the cost of upgrading RU equipment, particularly FPGA-based systems, to support these algorithms must be weighed against the possible risks to enable an informed, risk-based decision on where and how to best implement this type of solution.

11 CONCLUSION

Securing PTP in the S-plane within the Open RAN framework is essential, as demonstrated by our findings. Successful attacks can lead to severe disruptions, such as complete gNB outages requiring manual restoration, underscoring the need for robust security in multi-vendor environments that expand attack surfaces.

Addressing these threats involves balancing security costs against performance and financial implications. While robust measures like encryption introduce latency and computational overhead, TIMESAFE offers an effective solution. Our machine learning-based monitoring system achieves over 97.5% accuracy in detecting malicious attacks, providing a cost-efficient approach with minimal additional cost.

By using advanced machine learning techniques, TIMESAFE enables real-time detection of threats, allowing for targeted application of higher-cost security measures only when necessary. This adaptive strategy optimizes security and performance, highlighting the importance of tailored solutions to safeguard PTP synchronization in Open RAN networks. The demonstrated vulnerabilities in the FH call for proactive, cost-effective security measures to prevent significant network disruptions.

REFERENCES

- [1] M. Wong, A. Prasad, and A. C. Soong, "The Security Aspect of 5G Fronthaul," *IEEE Wireless Communications*, vol. 29, no. 2, pp. 116–122, 2022.
- [2] Common Public Radio Interface, "Common Public Radio Interface: eCPRI Interface Specification V2.0," Common Public Radio Interface, Tech. Rep., MAY 2019. [Online]. Available: http://www.cpri.info/downloads/eCPRI_v_2.0_2019_05_10c.pdf
- [3] O-RAN Working Group 4, "O-RAN Fronthaul Control, User and Synchronization Plane Specification v12," O-RAN.WG4.CUS.0-R003-v12.00, Tech. Rep., June 2023.
- [4] ETSI, "Publicly Available Specification (PAS); O-RAN Fronthaul Control, User and Synchronization Plane Specification v07.02; (O-RAN-WG4.CUS.0-v07.02)," ETSI TS 103 859 V7.0.2 (2022-09), Tech. Rep., 2022.
- [5] D. Dik and M. S. Berger, "Transport security considerations for the open-ran fronthaul," in *2021 IEEE 4th 5G World Forum (5GWF)*. IEEE, 2021, pp. 253–258.
- [6] A. S. Abdalla, P. S. Upadhyaya, V. K. Shah, and V. Marojevic, "Toward Next Generation Open Radio Access Networks—What O-RAN Can and Cannot Do!" *IEEE Network*, 2022.
- [7] C.-F. Hung, Y.-R. Chen, C.-H. Tseng, and S.-M. Cheng, "Security Threats to xApps Access Control and E2 Interface in O-RAN," *IEEE Open Journal of the Communications Society*, vol. 5, pp. 1197–1203, 2024.
- [8] T. O. Atalay, S. Maitra, D. Stojadinovic, A. Stavrou, and H. Wang, "Securing 5G OpenRAN with a Scalable Authorization Framework for xApps," in *IEEE INFOCOM 2023 - IEEE Conference on Computer Communications*, 2023, pp. 1–10.

- [9] K. Thimmaraju, A. Shaik, S. Flück, P. J. F. Mora, C. Werling, and J.-P. Seifert, "Security Testing The O-RAN Near-Real Time RIC & A1 Interface," in *Proceedings of the 17th ACM Conference on Security and Privacy in Wireless and Mobile Networks*, ser. WiSec '24. New York, NY, USA: Association for Computing Machinery, 2024, p. 277–287. [Online]. Available: <https://doi.org/10.1145/3643833.3656118>
- [10] J. Boswell and S. Poretsky, "Security considerations of Open RAN," *Stockholm: Ericsson*, 2020.
- [11] O-RAN Working Group 11, "Security Requirements Specifications," O-RAN.WG11.Security-Requirements-Specification.O-R003-v06.00, Tech. Rep., June 2023.
- [12] D. of Defense, "5G Strategy Implementation Plan," Department of Defense, Tech. Rep., December 2020, accessed: 2024-02-15. [Online]. Available: <https://apps.dtic.mil/sti/pdfs/AD1118833.pdf>
- [13] J. Groen, S. D'Oro, U. Demir, L. Bonati, D. Villa, M. Polese, T. Melodia, and K. Chowdhury, "Securing O-RAN Open Interfaces," *IEEE Transactions on Mobile Computing*, 2024.
- [14] E. Municio, G. Garcia-Aviles, A. Garcia-Saavedra, and X. Costa-Pérez, "O-RAN: Analysis of Latency-Critical Interfaces and Overview of Time Sensitive Networking Solutions," *IEEE Communications Standards Magazine*, vol. 7, no. 3, pp. 82–89, 2023.
- [15] A. Maamary, H. A. Alameddine, M. Debbabi, and C. Assi, "Synchronization plane in o-ran: Overview, security and research directions," *IEEE Communications Magazine*, pp. 1–7, 2024.
- [16] S. Shi, Y. Xiao, C. Du, M. H. Shahriar, A. Li, N. Zhang, Y. T. Hou, and W. Lou, "MS-PTP: Protecting Network Timing from Byzantine Attacks," in *Proceedings of the 16th ACM Conference on Security and Privacy in Wireless and Mobile Networks*, 2023, pp. 61–71.
- [17] "IEEE Standard for a Precision Clock Synchronization Protocol for Networked Measurement and Control Systems," *IEEE Std 1588-2019 (Revision of IEEE Std 1588-2008)*, pp. 1–499, 2020.
- [18] "NIST Special Publication 800-207: Zero Trust Architecture," 2020.
- [19] O-RAN Working Group 11, "O-RAN Security Threat Modeling and Risk Assessment," O-RAN.WG11.Threat-Modeling.O-R003-v03.0, Tech. Rep., 2024.
- [20] —, "O-RAN Security Test Specifications," O-RAN.WG11.SecTestSpecs.O-R003-v07.00, Tech. Rep., 2024.
- [21] M. Polese, L. Bonati, S. D'oro, S. Basagni, and T. Melodia, "Understanding O-RAN: Architecture, interfaces, algorithms, security, and research challenges," *IEEE Communications Surveys & Tutorials*, vol. 25, no. 2, pp. 1376–1411, 2023.
- [22] D. Dik and M. S. Berger, "Open-RAN fronthaul transport security architecture and implementation," *IEEE Access*, 2023.
- [23] J. Y. Cho and A. Sergeev, "Secure Open Fronthaul Interface for 5G Networks," in *Proceedings of the 16th International Conference on Availability, Reliability and Security*, ser. ARES 21. New York, NY, USA: Association for Computing Machinery, 2021.
- [24] J. Groen, S. D'Oro, U. Demir, L. Bonati, M. Polese, T. Melodia, and K. Chowdhury, "Implementing and evaluating security in O-RAN: Interfaces, Intelligence, and Platforms," *IEEE Network*, 2024.
- [25] "IEEE Standard for a Precision Clock Synchronization Protocol for Networked Measurement and Control Systems," *IEEE Std 1588-2019 (Revision of IEEE Std 1588-2008)*, pp. 1–499, 2020.
- [26] F. Rezabek, M. Helm, T. Leonhardt, and G. Carle, "PTP security measures and their impact on synchronization accuracy," in *2022 18th International Conference on Network and Service Management (CNSM)*. IEEE, 2022, pp. 109–117.
- [27] "Precision time protocol telecom profile for phase/time synchronization with full timing support from the network," *International Telecommunication Union Recommendation ITU-T G.8275.1/Y.1369.1*, 2022. [Online]. Available: <https://www.itu.int/rec/T-REC-G.8275.1-202211-I/en>
- [28] D. Dik, I. Larsen, and M. S. Berger, "MACsec and AES-GCM Hardware Architecture with Frame Preemption Support for Transport Security in Time Sensitive Networking," in *2023 International Conference on Computer, Information and Telecommunication Systems (CITS)*. IEEE, 2023, pp. 01–07.
- [29] D. Dik, R. Oliveira, E. Arabul, C. Vrontos, M. Berger, R. Nejabati, and D. Simeonidou, "100 Gbps multi-tenant FPGA-based MACsec aggregation to secure the open-RAN fronthaul," in *49th European Conference on Optical Communications (ECOC 2023)*, vol. 2023. IET, 2023, pp. 870–873.
- [30] C. DeCusatis, R. M. Lynch, W. Kluge, J. Houston, P. A. Wojciak, and S. Guendert, "Impact of cyberattacks on precision time protocol," *IEEE Transactions on Instrumentation and Measurement*, vol. 69, no. 5, pp. 2172–2181, 2019.
- [31] E. Itkin and A. Wool, "A security analysis and revised security extension for the precision time protocol," *IEEE Transactions on Dependable and Secure Computing*, vol. 17, no. 1, pp. 22–34, 2017.
- [32] E. Shereen, F. Bitard, G. Dán, T. Sel, and S. Fries, "Next steps in security for time synchronization: Experiences from implementing IEEE 1588 v2.1," in *2019 IEEE International Symposium on Precision Clock Synchronization for Measurement, Control, and Communication (ISPCS)*. IEEE, 2019, pp. 1–6.
- [33] B. Moussa, M. Debbabi, and C. Assi, "A detection and mitigation model for PTP delay attack in an IEC 61850 substation," *IEEE Transactions on Smart Grid*, vol. 9, no. 5, pp. 3954–3965, 2016.
- [34] B. Moussa, C. Robillard, A. Zugenmaier, M. Kassouf, M. Debbabi, and C. Assi, "Securing the precision time protocol (PTP) against fake timestamps," *IEEE Communications Letters*, vol. 23, no. 2, pp. 278–281, 2018.
- [35] B. Moussa, M. Kassouf, R. Hadjidj, M. Debbabi, and C. Assi, "An extension to the precision time protocol (PTP) to enable the detection of cyber attacks," *IEEE Transactions on Industrial Informatics*, vol. 16, no. 1, pp. 18–27, 2019.
- [36] A. Finkensteller, O. Butowski, E. Regnath, M. Hamad, and S. Steinhorn, "PTPsec: Securing the Precision Time Protocol Against Time Delay Attacks Using Cyclic Path Asymmetry Analysis," *arXiv preprint arXiv:2401.10664*, 2024.
- [37] NIS Cooperation Group, "Report on the cybersecurity of Open RAN," Tech. Rep., 2022. [Online]. Available: <https://digital-strategy.ec.europa.eu/en/library/cybersecurity-open-radio-access-networks>
- [38] IBM, "IBM X-Force Cloud Threat Landscape Report 2023," IBM Corporation, Tech. Rep., 2023. [Online]. Available: <https://www.ibm.com/downloads/cas/QWBXVAPL>
- [39] C. D. Hylender, P. Langlois, A. Pinto, and S. Widup, "2024 Data Breach Investigations Report," Verizon Business, Tech. Rep., 2024. [Online]. Available: <https://www.verizon.com/business/resources/Tce6/reports/2024-dbir-data-breach-investigations-report.pdf>
- [40] J. Xing, S. Yoo, X. Foukas, D. Kim, and M. K. Reiter, "On the Criticality of Integrity Protection in 5G Fronthaul Networks," in *33rd USENIX Security Symposium (USENIX Security 24)*, 2024, pp. 4463–4479.
- [41] W. Tiberti, E. Di Fina, A. Marotta, and D. Cassioli, "Impact of man-in-the-middle attacks to the o-ran inter-controllers interface," in *2022 IEEE Future Networks World Forum (FNWF)*. IEEE, 2022, pp. 367–372.
- [42] F. Klement, A. Brighente, M. Polese, M. Conti, and S. Katzenbeisser, "Securing the open ran infrastructure: Exploring vulnerabilities in kubernetes deployments," in *2024 IEEE 10th International Conference on Network Softwarization (NetSoft)*, 2024, pp. 185–189.
- [43] D. Villa, I. Khan, F. Kaltenberger, N. Hedberg, R. S. da Silva, A. Kelkar, C. Dick, S. Basagni, J. M. Jornet, T. Melodia *et al.*, "An Open, Programmable, Multi-vendor 5G O-RAN Testbed with NVIDIA ARC and OpenAirInterface," *Proc. of the 2nd IEEE Workshop on Next-generation Open and Programmable Radio Access Networks (NG-OPERA)*, 2024.
- [44] OpenAirInterface Software Alliance. [Online]. Available: <https://openairinterface.org>
- [45] OnePlus. [Online]. Available: <https://www.oneplus.com/us/nord-specs>
- [46] A. Masaracchia, V. Sharma, M. Fahim, O. A. Dobre, and T. Q. Duong, "Digital Twin for Open RAN: Toward Intelligent and Resilient 6G Radio Access Networks," *IEEE Communications Magazine*, vol. 61, no. 11, pp. 112–118, 2023.
- [47] M. Polese, L. Bonati, S. D'Oro, P. Johari, D. Villa, S. Velumani, R. Gangula, M. Tsampazi, C. P. Robinson, G. Gemmi *et al.*, "Colosseum: The open ran digital twin," *arXiv preprint arXiv:2404.17317*, 2024.
- [48] J. Groen, B. Kim, and K. Chowdhury, "The Cost of Securing O-RAN," in *ICC 2023-IEEE International Conference on Communications*. IEEE, 2023, pp. 5444–5449.
- [49] [Online]. Available: <https://nvd.nist.gov/vuln-metrics/cvss/v3-calculator>
- [50] Rapid7 Global Consulting, "Under the hoodie, lessons from a season of penetration testing," Rapid7, Tech. Rep., 2018. [Online]. Available: https://www.rapid7.com/globalassets/_pdfs/research/rapid7-under-the-hoodie-2018-research-report.pdf
- [51] I. Afolabi, T. Taleb, K. Samdanis, A. Ksentini, and H. Flinck, "Network slicing and softwarization: A survey on principles, enabling technologies, and solutions," *IEEE Communications Surveys*

& *Tutorials*, vol. 20, no. 3, pp. 2429–2453, 2018.

- [52] W.-H. Ko, U. Ghosh, U. Dinesha, R. Wu, S. Shakkottai, and D. Bharadia, “EdgeRIC: Empowering real-time intelligent optimization and control in NextG cellular networks,” in *21st USENIX Symposium on Networked Systems Design and Implementation (NSDI 24)*, 2024, pp. 1315–1330.
- [53] J. Xing, J. Gong, X. Foukas, A. Kalia, D. Kim, and M. Kotaru, “Enabling Resilience in Virtualized RANs with Atlas,” in *Proceedings of the 29th Annual International Conference on Mobile Computing and Networking*, 2023, pp. 1–15.
- [54] N. Lazarev, T. Ji, A. Kalia, D. Kim, I. Marinou, F. Y. Yan, C. Delimitrou, Z. Zhang, and A. Akella, “Resilient Baseband Processing in Virtualized RANs with Slingshot,” in *Proceedings of the ACM SIGCOMM 2023 Conference*, 2023, pp. 654–667.



Joshua Groen received the BSE degree in electrical engineering from Arizona State University, in 2007, and the MS degree in electrical engineering from the University of Wisconsin, in 2017. He is currently working toward the PhD degree with Northeastern University. His research interests include wireless communications, security, and machine learning. Previously he worked with the US Army Regional Cyber Center – Korea as the senior network engineer.



Simone Di Valerio received the BSE degree in Computer Science from Sapienza University of Rome, in 2021, and will receive the MS degree in Cybersecurity from Sapienza University of Rome in January 2025.



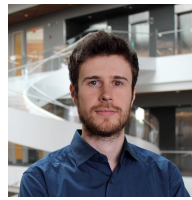
Imtiaz Karim is a Postdoctoral Researcher in the Department of Computer Science at Purdue University. He received the Ph.D. degree from the same department in Spring 2023. His research interests include systems and network security, with a particular focus on analyzing the security and privacy of wireless communication protocols.



Davide Villa received the BS degree in computer engineering, and the MS degree in embedded computing systems from the University of Pisa and Sant’Anna School of Advanced Studies, in 2015 and 2018, respectively. He is currently working toward the PhD degree with Northeastern University. His research interests focus on 5G-and-beyond cellular networks, software-defined networking, O-RAN, and channel modeling.



Yiewi Zhang is pursuing the Ph.D. degree in computer science at Purdue University, which she began in August 2022. She received the M.S. degree in computer science from Shanghai Jiao Tong University, in 2022, and the B.S. degree in information security from Xidian University, in 2019.



Leonardo Bonati received the PhD degree from Northeastern University, in 2022. He is an associate research scientist with Northeastern University. His research focuses on softwareized NextG systems.



Michele Polese received the PhD degree from the University of Padova, in 2020. He is a research assistant professor with Northeastern University. His research focuses on architectures for wireless networks.



Salvatore D’Oro received the PhD degree from the University of Catania, in 2015. He is a research assistant professor with Northeastern University. He serves on the Technical Program Committee of IEEE INFOCOM. His research focuses on optimization and learning for NextG systems.



Tommaso Melodia received the PhD degree from the Georgia Institute of Technology, in 2007. He is the William Lincoln Smith professor with Northeastern University, the director of the Institute for the Wireless Internet of Things, and the director of research for the PAWR Project Office. His research focuses on wireless networked systems.



Elisa Bertino received the Ph.D. degree in computer science from the University of Pisa, in 1980. She is the Samuel D. Conte Distinguished Professor of Computer Science at Purdue University. Her research focuses on security of cellular networks, mobile applications and IoT systems, zero-trust architectures, and machine learning techniques for cybersecurity.



Francesca Cuomo received the Ph.D. degree in information and communications engineering from Sapienza University of Rome, in 1998. She is a Full Professor with Sapienza University, where she has taught courses in telecommunication networks since 2005.



Kaushik Chowdhury received the PhD degree from the Georgia Institute of Technology, in 2009. He is a Chandra Family Endowed Distinguished Professor in Electrical and Computer Engineering at The University of Texas at Austin. His current research interests involve systems aspects of machine learning for agile spectrum sensing/access, unmanned autonomous systems, programmable and open cellular networks, and largescale experimental deployment of emerging wireless technologies.